Elevated urine BMPs - bis(Monoacylglycerol)Phosphates – in LRRK2 G2019S, R1441G/C and VPS35 D620N mutation carriers with and without Parkinson's disease

Sara Gomes[1], Alicia Garrido[2,3,4], Francesca Tonelli[1],Donina Obiang[2,3], Eduardo Tolosa[3,4], Maria Jose Marti[2,3,4], Javier Ruiz-Martinez[5], Ana Vinagre Aragon[5], Haizea Hernandez-Eguiazu[5], Ioana Croitoru[5], Vicky L Marshall[6], Theresa Koenig[7], Christoph Hotzy[7], Frank Hsieh[8], Marianna Sakalosh[8], Elizabeth Tengstrand[8], Shalini Padmanabhan[9], Kalpana Merchant[10], Christof Bruecke[11], Walter Pirker[12], Alexander Zimprich[7], Esther Sammler[1,12]

1 Medical Research Council Protein Phosphorylation and Ubiquitylation Unit, University of Dundee, Dundee DD1 5EH, UK

2 Parkinson's Disease and Movement Disorders Unit, Institut Clínic de Neurociències, Hospital Clinic de Barcelona, Barcelona, Spain.

3 Department of Clinical and Experimental Neurology, Laboratory of Parkinson disease and other Neurodegenerative Movement Disorders: Clinical and Experimental Research, IDIBAPS, University of Barcelona, Barcelona, Spain

4 Centre for Networked Biomedical Research on Neurodegenerative Diseases (CIBERNED), Madrid, Spain.

5 Group of Neurodegenerative Diseases, Biodonostia Research Institute, San Sebastian, Spain

6 Neurology, Queen Elizabeth University Hospital, Institute of Neurological Sciences, Glasgow, UK

7 Department of Neurology, Medical University of Vienna, Währinger Gürtel 18-20, 1090 Wien, Austria.

8 Nextcea, Inc. 500 West Cummings Park, Suite 4550, Woburn, Massachusetts, USA

9 The Michael J. Fox Foundation for Parkinson's Research, New York, NY, USA

10 TransThera Consulting Co, Portland, USA

11 Department of Neurology, Klinik Ottakring, Vienna, Austria

12 Molecular and Clinical Medicine, Ninewells Hospital and Medical School, University of Dundee, Dundee DD1 9SY, UK

Corresponding author:

Esther Sammler MD PhD

e.m.sammler@dundee.ac.uk

Word count: 4047

Abstract word count: 244

Abstract

Background: Parkinson's disease is the second most common neurodegenerative condition and has no cure. With the emergence of targeted treatments such as LRRK2 small molecule inhibitors that are currently being evaluated in clinical trials there is an urgent need for patient stratification and target engagement biomarkers. Urine BMP (didocohexaenoyl (22:6) bis(monoacylglycerol)phosphate) levels have previously been reported to be elevated in gain-of-kinase function LRRK2 G2019S mutation carriers and reduced in LRRK2 knockout mice, as well as non-human primates treated with LRRK2 kinase inhibitors.

Objective: The purpose of this study was to independently validate and expand our understanding of urine BMPs as a PD biomarker in carriers of LRRK2 G2019S but also LRRK2 R1441 hotspot mutations, VPS35 D620N and GBA variants compared to idiopathic PD and control subjects.

Methods: Up to 20 BMP species including total and 2,2'- isoforms of the di-18:1-BMP and di-22:6-BMP species were measured in urine from 106 participants: 22 controls, 31 with iPD, 10 with PD associated with GBA risk variants, as well as 18 LRRK2 G2019S, 13 LRRK2 R1441G/S and 10 VPS35 D620N mutation carriers either with or without PD.

Results: Urine BMP levels were consistently elevated in carriers of LRRK2 G2019S and R1441G/C as well as VPS35 D620N mutations, but not those carrying GBA risk variants.

Conclusion: Urine BMP levels are attractive and promising biomarkers for patient stratification in PD and potentially target engagement in clinical trials. Our results further highlight the convergence of the LRRK2 and VPS35 signalling pathways.

Introduction

Parkinson's disease (PD) is the most common neurodegenerative movement disorder affecting about 6 million people worldwide with numbers expected to rise and with no cure[1]. While the aetiology of most cases of PD is poorly understood (e.g. idiopathic), rarer monogenetic, inherited forms have advanced our understanding of PD and the development of disease-modifying treatments that are currently being evaluated in clinical trials[2]. One such example is the leucine-rich repeat kinase 2 (LRRK2) as several lines of evidence support the therapeutic potential of LRRK2 kinase inhibitors in PD: pathogenic LRRK2 variants are relatively common causing 1-3% of all cases of PD, resemble idiopathic PD (iPD) and result in increased LRRK2 kinase activity with subsequent hyperphosphorylation of its endogenous Rab GTPase substrates including Rab10[3 4]. While studying the downstream effects of LRRK2 substrate phosphorylation can shed light on its diverse cellular functions[5-7], LRRK2 dependent Rab phosphorylation can also serve as a biomarker for LRRK2 kinase activation status and target engagement in peripheral blood using quantitative immunoblotting and more sensitive targeted mass-spectrometry approaches[8 9]. Increased LRRK2-dependent Rab10 phosphorylation has been demonstrated in carriers of the pathogenic LRRK2 R1441G as well as the PD causing VPS35 D620N variants but not LRRK2 G2019S[10 11]. The latter can be explained by modest activating effect of the G2019S mutation – under 2-fold activation of LRRK2 kinase activity in homozygous knock-in animals as compared to over 4-6-fold with the R1441 hotspot and VPS35 D620N mutations[4 11 12], in addition to the intrinsic variability when working with clinical samples resulting in unfavourable signal to noise ratio. In addition to peripheral blood, urine has shown promise for biomarker discovery and patient stratification in PD: Recent urine proteomic studies have revealed a lysosomal dysregulation signature[13] and elevated bis(monoacylglycero)phosphate (BMP) levels[14] in LRRK2 G2019S mutation carriers. The latter is consistent with previous observations of decreased BMPs in urine of *lrrk2* knockout mice, and non-human primates treated with LRRK2 kinase inhibitors[15]. Interestingly in the nonhuman primate study, levels of BMP in the kidney cortex

were significantly elevated with LRRK2 inhibitors suggesting that LRRK2 is regulating the secretion of BMP from the kidney[16]. It has also been reported that treatment with the DNL201 LRRK2 inhibitor resulted in a marked decrease in urine BMP levels in 122 healthy volunteers and in 28 patients with PD in phase 1 and phase 1b clinical trials respectively[16]. BMPs belong to a broad group of atypical, negatively charged phospholipids important for membrane formation and function in the endosome-lysosome compartment, including intraluminal vesicles (ILV) and extracellularly released exosomes[17].

The aim of this study was to independently validate and expand our understanding of urine BMP levels as a biomarker for enhanced LRRK2 pathway activity and endolysosomal dysfunction in LRRK2 G2019S as well as LRRK2 R1441G/C, VPS35 D620N and GBA mutation carriers in comparison to iPD and controls. Our results highlight that urine BMPs are consistently elevated in carriers of both LRRK2 G2019S and R1441G/C as well as VPS35 D620N mutations, but not those carrying GBA risk variants. A moderate increase for some BMP species was also observed within the iPD group. Taken together, our data add further evidence of convergence of the LRRK2 and VPS35 signalling pathways and the utility of urine BMP levels as an easily accessible biomarker for endolysosomal trafficking defects.

Materials and Methods

Study participants

106 participants across 4 different sites were recruited for this study between 2019 and 2021 including 33 individuals via the Movement Disorder Clinics at the Hospital Clinic Universitari de Barcelona, Spain, 28 via Klinik Ottakring and the University Hospital in Vienna, Austria, 33 via the Neurology Department at Ninewells Hospital and Medical School, Dundee, UK, and 12 via the Hospital Universitario Donostia in San Sebastian, Spain. Controls were self-reported in general good health, did not have a diagnosis or family history of PD or tremor and did not suffer from any other neurodegenerative conditions. Demographic information including age at study participation, sex, as well as disease duration and age at PD onset where applicable was also collected (Supplementary table 1).

Genotyping:

Mode of genetic testing varied across sites. In Dundee, all participants with PD underwent sequencing of the LRRK2 and GBA genes - the exceptions were the ATP13A2 mutation and SNCA duplication carriers who were investigated by PD gene panel testing of over 20 PD associated genes. In Vienna, participants with iPD and GBA variant carriers underwent exome sequencing while carriers of the VPS35 D620N mutation were investigated with Sanger sequencing specifically for VPS35 D620N as they were all related to cases in the original report identifying the VPS35 D620N mutation as a cause of PD by next generation sequencing[18]. In Barcelona, genotyping of the G2019S variant was performed on a StepOnePlus Real-Time PCR System (Life Tech. Inc) using the commercial pre-designed TaqMan assay C-63498123-10 SNP rs 34637584 while TaqMan assay on demand was used for identifying the R1441 variant. No other mutations were tested. Also in San Sebastian, only targeted testing for the G2019S and R1441 hotspot mutations was performed.

Urine collection

Fresh midstream urine was collected and analysed from participants in Barcelona and Vienna in 2019 and from participants in San Sebastian and Dundee in 2020/2021 with analysis performed in 2021. Up to 10 ml of urine was centrifuged for 15 minutes at 2500 x g and 4°C in most cases within

half an hour from collection. The supernatant was transferred and aliquoted into labelled tubes and immediately snap frozen, and maintained at -80°C for storage and shipment, until analysis at Nextcea, Inc.

Ethical approval and consent to participate

The study was approved by the respective local ethics committees. All participants gave written informed consent.

Quantitative Ultra Performance Liquid Chromatography Tandem Mass Spectrometry (UPLC MS/MS) analyses

A multiplexed UPLC-MS/MS method was used to simultaneously quantitate molecular species of BMPs in urine. The individual phospholipids included BMP species with 22:6/22:6, 18:1/18:1, 18:1/22:6, 18:2/22:6, 18:2/18:2, 18:1/18:2, 20:4/22:6, 18:2/20:4, 16:0/18:2, and 18:0/18:1 fatty acid chains. Analyses of the 10 lipids were performed by Nextcea, Inc. (Woburn, MA) in a single acquisition. Standard curves were prepared from authentic di-22:6-BMP and di-18:1-BMP standards. Di-22:6-BMP-d5 was used as an internal standard for quantitation. Concentrations of urine BMPs were quantitated using a SCIEX 7500 UPLC MS/MS System controlled with SCIEX OS 2.0 software.

Measurement of urinary 2,2'-di-22:6-BMP, 2,3'-di-22:6-BMP, 3,3'-di-22:6-BMP, total di 22:6-BMP, 2,2'-di-18:1-BMP, 2,3'-di-18:1-BMP, 3,3'-di-18:1-BMP and total di 18:1-BMP

BMPs can exist in three geometrical isoforms (2, 2'-, 2, 3'-, and 3, 3'- BMP), which may influence their functional properties. Targeted UPLC-MS/MS using multiple reaction monitoring was used to absolutely quantitate total di-22:6-BMP (the sum of its three isoforms) and its distinct 2,2'-, 2,3'-, and 3,3'-isoforms (2,2'-di-22:6-BMP, 2,3'-di-22:6-BMP, and 3,3'-di-22:6-BMP). Total di-18:1-BMP, 2,2'-di-18:1-BMP, 2,3'-di-18:1-BMP, and 3,3'-di-18:1-BMP were measured as well. Quantitation was performed by Nextcea, Inc. (Woburn, MA) using authentic di-22:6-BMP and di-18:1-BMP reference standards. Di-22:6-BMP-d5 was employed as an internal standard. BMPs in urine were extracted by liquid-liquid extraction and measured by UPLC-MS/MS as described above.

Data was acquired for 7 BMP isoforms for all participants (n=104 – 106), 8 for urines measured in 2019 (n=85) and 4 exclusively for urines measured in 2021 (n=25 – 38).

Calibration and data processing

The intensities of the analytes and internal standard were determined by integration of extracted ion peak areas using SCIEX OS software. Calibration curves were prepared by plotting the peak area ratios for each analyte to the internal standard versus concentration. The model for the calibration curve was linear with (1/x2) weighting. Measured concentrations of urine BMPs (ng/mL) were divided by urine creatinine and reported in ng/mg creatinine.

Creatinine measurements

Concentrations of urine creatinine were measured by colorimetric assay (method of Jaffé) with Parameter Creatinine Assay test reagents (R&D Systems, Minneapolis, MN) using a BioTek Synergy LX microplate reader with Gen5 Microplate Reader and Imager Software 2.09 (Fisher Scientific, Hampton, NH).

Data analysis and data availability

All data analysis was carried out in R (version 4.1.2). After data checking and cleaning, exploratory analysis was carried out by calculating descriptive statistics and plotting the variables. Data were checked for normal distribution by plotting histograms and q-q plots. As BMPs were found not to follow a normal distribution, non-parametric statistical tests (Kruskal-Wallis with post-hoc Dunn's test) were used to compare the 6 groups we have defined: control, iPD, LRRK2 G2019S, LRRK2 R1441G/C, VPS35 D620N, and GBA. Adjusted *p* values are reported (*p* values lower than 0.001 are reported as $p < 0.001$), and $p < 0.05$ was considered statistically significant, in accordance with SAMPL guidelines[19].

To assess the potential impact of sex and age as predictors of variance of BMP levels, generalised linear models were applied. For this, each measured BMP species was log-transformed and taken as a response variable. The maximal model was calculated including experimental group, sex, and age as covariates. This was reduced to a minimum sufficient model by sequential removal of terms with highest p-value and lowest AIC (Akaike information criterion). The behaviour of residuals was checked by plotting and the models were considered valid only if residuals showed constant variation across the range as well as normal distribution. For assessing the correlation between the different BMP species, the log-transformed BMP levels were plotted pairwise in scatterplots, and the Pearson correlation coefficient was determined.

Results

Clinical cohort

Urine was collected from 106 participants across 4 sites including 22 healthy controls, 31 individuals with iPD, and the following carriers of heterozygous pathogenic variants: 18 with the LRRK2 G2019S mutation (11 PD/7 non-manifesting carriers (NMC)), 13 with LRRK2 R1441G/C mutation (7 PD/6 NMC) and 10 with the pathogenic VPS35 D620N mutation (1 of whom was a NMC), as well as 10 individuals with PD associated with various GBA risk variants. Additionally, one participant with PD and a SNCA duplication and one participant with atypical young onset PD due to a novel homozygous ATP13A2 G38D mutation were included in this study. Table 1 gives an overview of participants' demographics, clinical status with regards to PD and genotype according to groups. While our groups were balanced for sex, the mean age of the control group was significantly younger compared to the LRRK2 G2019S, LRRK2 R1441G/C, and iPD but not compared to the GBA or VPS35 D620N groups.

BMP isoforms are significantly raised in LRRK2 G2019S, R1441G/C and VPS35 D620N mutation carriers

The broad profiling of up to 20 urine BMP isoforms normalized to urine creatinine for all available participants is reported in supplementary table 1. Table 1 and figure 1 show the data for the total and 2,2'- isoforms of the di-18:1-BMP and di-22:6-BMP species that had previously been reported to most strongly discriminate between LRRK2 G2019S mutation carriers and non-carriers. All of these BMP isoforms were significantly raised in the LRRK2 G2019S mutation carrier group when compared to controls: over 6-fold for urinary 2,2'-di-22:6 BMP levels (adjusted $p < 0.001$), 5.7-fold for 2,2'-di-18:1-BMP (adjusted $p < 0.001$), 5.2-fold for total 22:6 BMP (adjusted $p < 0.001$), and over 3.5-fold for total di-18:1-BMP (adjusted $p < 0.001$). A similarly significant increase in BMP levels compared to controls was also seen in the VPS35 D620N and LRRK2 R1441G/C mutation carrier groups (figure 1). No statistically significant difference compared to controls was observed for the GBA risk variant group. With regards to iPD, a statistically significant increase with an effect size of around 2-fold was

seen for 2,2'-di-18:1-BMP (adjusted p=0.024), total di-18:1-BMP (adjusted p=0.005), and 2,2'-di-22:6-BMP (adjusted p=0.02) when compared to controls, while no statistically significant difference was found for total di-22:6-BMP (adjusted p=0.072). While the BMP levels of the participants with the homozygous ATP13A2 mutation and the SNCA duplication were not included in any of the grouped analyses, the BMP levels for the SNCA duplication carrier were close to median of the control group. For the ATP13A2 mutation carrier, all BMP isoforms were high, in particular the total and 2,2'-di-18:1 isoforms, which were more than 3-fold higher than the upper range of the LRRK2 G2019S group.

No significant difference between manifesting and non-manifesting LRRK2 mutation carriers

For each of the total and 2,2'-di-18:1 and -di-22:6 BMP isoforms, Kruskal Wallis testing was performed to assess whether there are significant differences between PD manifesting and non-manifesting carriers for the LRRK2 G2019S and R1441G/C mutation carriers. We found that BMP levels did not significantly differ between LRRK2 mutation carriers with or without a clinical diagnosis of PD (supplementary table 2). Given that there was only one non-manifesting carrier amongst the VPS35 D620N group and all GBA risk variant carriers had a diagnosis of PD, these groups were not included in the analysis to look at the effect of disease status.

Overall group comparisons for total and 2,2'-di-18:1 and -di-22:6 BMP isoforms

Figure 1 shows that BMP species tended to be higher in LRRK2 G2019S mutation carriers compared to LRRK2 R1441G/C mutation carriers, but this was only statistically significant for total di-18:1-BMP and not 2,2'-di-18:1-BMP or total and 2,2'-di-22:6-BMPs, using Kruskal-Wallis test with post-hoc Dunn test for multiple comparisons (supplementary table 3). For total and 2,2'-di-18:1-BMPs, VPS35 D620N mutation carriers tended to have higher levels than both LRRK2 G2019S and R1441G/C mutation carriers, but this only reached statistical significance for total di-18:1-BMP (VPS35 D620N *vs* R1441G/C, adjusted p=0.029). All other group comparisons are also listed in supplementary table 3.

Correlation between BMP species and impact of sex and age

We next performed a correlation analysis for the 2,2'-di-18:1, total di-18:1, 2,2'-di-22:6 and total di-22:6 BMP isoforms and found good correlation between the 2,2'- and total values for both the 18:1 (R=0.966) and 22:6 BMP (R=0.985) species (supplementary figure 1). Moving forward, we used the total di-18:1 and total di-22:6 BMP species to determine the impact of age and sex. Total di-18:1-BMP and total di-22:6-BMP were modelled as general linear models, considering age, sex, and genotype as covariates. Regarding total di-18:1-BMP, neither the age ($p = 0.0622$) nor the sex ($p = 0.1273$) covariates were statistically significant and were therefore considered not to be predictors of the observed BMP variation. Conversely, the genotype covariate displayed a statistically significant effect ($p < 0.001$) on total di-18:1-BMP, with significant differences in the iPD group, as well as in both LRRK2 mutation carrier groups and VPS35 mutation carriers. Similarly, the sex covariate did not show a statistically significant effect on di-22:6-BMP variation (p=0.864), although age did in this instance ($p = 3.65\times10^{-5}$). Nonetheless, even after adjusting for age, the genotype was also a predictor for total di-22:6-BMP variation, with significant differences observed for LRRK2 G2019S, R1441G/C and VPS35 D620N. The same linear model was applied to 2,2'-di-18:1-BMP and 2,2'-di-22:6-BMP with the same outcome as for the respective total species (data not shown).

Additional BMP isoforms

Table 2 provides values for BMP analytes with median, range and available data points for the different group, as well as p-values for Kruskal-Wallis test used to assess overall differences across the groups. Some analytes were not available for all participants, as outlined in the methods section, but additionally, some measurements were below quantification levels – 38 out of 68 for BMP-18:0/20:4, 27, 22, and 21 out of 106 for BMP-16:0/18:2, BMP-18:2/20:4, and BMP-20:4/22:6 respectively, 13 out of 38 for 3,3'-BMP-18:1, and 2 out of 106 for BMP-18:2/22:6. As with the total and 2,2'-di-18:1- and di-22:6 BMP isoforms, there was a statistically significant difference between the control and LRRK2 G2019S mutation carrier groups for all additional BMP species (Supplementary Figure 2), excluding those where sample size did not allow for analysis – either because only 2 measurements were available for the control (18:0/20:4) or the LRRK2 G2019S mutation carrier groups (2,3-BMP-18:1, 2,3-BMP-22:6, 3,3'-BMP-22:6, and 3,3'-BMP-18:1). All species that were significantly increased in the LRRK2 G2019S group were also significantly increased in LRRK2 R1441G/C and VPS35 D620N mutation carriers compared to the control group. For iPD, there was a statistically significant increase of 4 species (BMP-18:1/22:6, BMP-18:2, BMP-18:1/18:2 and BMP-18:2/22:6), but not for 7 other species. As before, there was no significant difference for any of the BMP isoforms between the GBA risk variant group and controls.

Discussion

At a time of rising cases of PD and emerging disease-modifying treatments, reliable biomarkers that reflect underlying disease mechanisms and have potential for target engagement studies are urgently needed. We and others have previously highlighted the utility of LRRK2 substrate phosphorylation, e.g. LRRK2-dependent Rab10 phosphorylation at threonine 73, in peripheral blood as a biomarker for LRRK2 kinase activity. We have shown that LRRK2-dependent Rab10 phosphorylation is significantly elevated in human peripheral blood neutrophils derived from heterozygous LRRK2 R1441G mutation carriers with and without PD[10] – in keeping with the 3-4-fold activation of the LRRK2 kinase in cellular and knock-in animal models of LRRK2 R1441 hotspot mutations [3 20 21]. An even greater effect on LRRK2-dependent Rab10 phosphorylation is seen with the VPS35 D620N mutation that enhances LRRK2 kinase pathway activity in mice and human by a yet unknown mechanism[11]. On the other hand, the common G2019S mutation that resides in the kinase domain of LRRK2 and causes only modest, under 2-fold increase in LRRK2-dependent Rab10 phosphorylation in cellular and homozygous knock-in animal models, foregoes clear discrimination in peripheral blood of heterozygous mutation carriers. Only one study so far has shown increased Rab10 phosphorylation at threonine 73 in peripheral blood mononuclear cells (PBMCs) of LRRK2 G2019S mutation carriers, but only when corrected for reduced LRRK2 expression levels[22], which could also be due to the lack of LRRK2 expression in most cell types that constitute PBMCs. As such, there is a need for more sensitive and complementary assays, in particular for the LRRK2 G2019S mutation. Our data together with previous results[16 23] indicates that elevated urine BMP levels are a strong indicator of elevated LRRK2 signalling pathway activity. Urine collection is non-invasive and much easier to process in contrast with peripheral blood, which requires more specialized methodologies, and is also more time consuming and prone to technical error[9 11 24]. We were therefore interested to independently validate increased urine BMP levels in LRRK2 G2019S mutation carriers and expand the analysis to other mutations in LRRK2 and other PD genes mapping into endolysosomal biology.

In our study, we observed a significant increase in all BMP isoforms measured for LRRK2 G2019S mutation carriers irrespective of sex, age and PD status, confirming previous results[23]. We did not see a significant difference between PD manifesting compared to non-manifesting LRRK2 G2019S carriers (NMC) but caution needs to be exercised given the relatively small group size (11 PD/7 NMC). For example, the previous study was only able to observe a small but statistically significant increase in BMP levels in LRRK2 G2019S mutation carriers with PD after combining the results of 2 cohorts (45 PD/36 NMC) but not separately[23]. Additionally, we found a significant elevation in all BMP species measured for carriers of the LRRK2 R1441G/C as well as VPS35 D620N mutations when compared to controls, but not for GBA mutation carriers. As with LRRK2 G2019S, there was no significant difference between manifesting and non-manifesting carriers for LRRK2 R1441G/C but again with relatively small numbers (7 PD/6 NMC). Segregation analysis for manifesting and non-manifesting carriers was not attempted for the VPS35-D620N mutation as the group included only 1 NMC and neither for GBA as all GBA risk variant carriers had a clinical diagnosis of PD. Interestingly, BMP levels tended to be higher in LRRK2 G2019S mutation carriers compared to LRRK2 R1441G/C and also VPS35 D620N carriers, but this was only statistically significant for total di-18:1-BMP (p=0.031) and not for 2,2'-di-18:1-BMP and total/2,2'-di-22:6 BMPs. This trend is opposite to what is observed with regards to LRRK2 kinase activity where the effect size is larger in LRRK2 R1441G/C mutation carriers.

Importantly, as with LRRK2 dependent Rab10 phosphorylation, our results provide further evidence that kinase activating mutations in LRRK2 and the VPS35 D620N mutation operate in a shared pathway regulating endosomal-lysosomal and Golgi-sorting processes that result in elevated urine BMPs in humans[25]. However, despite the known greater effects of the LRRK2 R1441G/C and VPS35 D620N mutations on LRRK2 kinase activation in comparison to LRRK2 G2019S, urine BMP elevation did not follow the same pattern as urine BMP levels tended to be higher in LRRK2 G2019S compared to LRRK2 R1441G/C and to some degree also VPS35 D620N. GBA on the other hand encodes for a lysosomal hydrolase involved in the metabolism of glucosylceramide[26], which likely plays a distinct role in the secretory pathway without directly affecting membrane trafficking. This could explain why urine BMP levels were not elevated in the GBA mutation carriers in our study. It will be interesting to validate this in much larger datasets such as in the Parkinson's Progression Marker Initiative (PPMI)[27]. We obtained urine BMP data for one individual with the atypical PD syndrome Kufor-Rabek syndrome with novel homozygous mutations in ATP13A2 displaying significantly elevated urine BMPs that for the total and 2,2'-di-18:1-BMP species were much higher than for any other sample measured (supplementary table 1). ATP13A2 encodes a transmembrane endolysosomal ATPase that transports polyamines into the cell regulating endolysosomal cargo-sorting and proteostasis through an interaction with the BMP precursor phosphatidylinositol[28]. On the other hand, another individual with PD and alpha-synuclein duplication displayed urine BMP levels in the range of the control group. A finding that contrasted with the previous study[14] was that urine BMP levels were increased in our iPD group compared to controls and we hypothesize that this is more a reflection of the heterogeneity amongst individuals with iPD in itself, which highlights the need for mechanistic stratification in PD patients. However, not all BMP isoforms yielded a significant difference between the iPD and control groups and if so with a much lower calculated probability – for example, for total di-22:6-BMP, there was no statistically significant difference between iPD and controls, while total di-18:1-BMP was significantly increased in the iPD group (adjusted p=0.005). The adjusted p values for LRRK2 G2019S mutation carriers compared to controls

were much lower (adjusted $p < 0.001$ for total di-22:6-BMP and di-18:1-BMP). In future work it would be interesting to investigate whether iPD patients displaying elevated di-18:1-BMP levels could be taken as an indication of increased LRRK2 kinase pathway activity.

Alcalay et al. measured 54 distinct bioactive phospholipids from 3 classes - BMPs, cell membrane phospholipids, and globotriaosylceramides – and found that total di-18:1-BMP and total di-22:6-BMP most strongly discriminated LRRK2 G2019S mutation carriers from non-mutation carriers. The focus of our study was therefore on the total and 2,2'- species for both di-18:1-BMPs and di-22:6-BMPs species, for which we were able to obtain complete datasets. We found good correlation between the 2,2'- and total analytes for both the di-18:1- and di-22:6-BMP isoforms (supplementary figure 1). The additional BMP species measured in our study confirmed the same trend with significant elevation in carriers of both LRRK2 G2019S and R1441G/C, as well as VPS35 D620N mutations compared to control, and no significant change for GBA variant carriers compared to controls. Together, this data provides a framework for future studies and the potential consideration to narrow down the analysis of BMP species to the di-18:1- and di-22:6-BMP isoforms. Given that our cohort size per group was relatively small, we did not attempt correlating our data with any clinical PD parameters. As before, the BMP signature was mainly driven by genotype clearly demonstrating the value of urine BMP isoforms as a biomarker for dysfunctional endolysosomal trafficking such as with PD associated mutations in LRRK2 and VPS35 and previously reported lysosomal storage disorders. The observation that urine BMP levels in macaques as well as humans show a reduction upon chronic treatment with a LRRK2 kinase inhibitor that normalized after a wash out period[16 29], is consistent with the notion that secretion of BMP isoforms from the kidney to urine is controlled by the LRRK2 pathway.

In conclusion, we provide confirmation that urine BMP isoforms measured by mass spectrometry are robustly elevated in carriers of the LRRK2 G2019S mutation. Additionally, we provide first time evidence that urine BMPs are also elevated in LRRK2 R1441G/C and VPS35 D620N mutation carriers, consistent with shared biological pathways involved in endolysosomal trafficking. The observation that PD patients carrying GBA risk variants did not show a statistically significant difference in urine BMP levels compared to controls will need to be replicated in independent larger cohorts, but underlines that there are discriminatory biomarkers for patient stratification that may in the future assist in matching patients with the best available targeted treatments.

References

1. Dorsey ER, Sherer T, Okun MS, et al. The Emerging Evidence of the Parkinson Pandemic. *J Parkinsons Dis* 2018;8(s1):S3-S8. doi: 10.3233/JPD-181474 [published Online First: 2018/12/26]
2. Sardi SP, Cedarbaum JM, Brundin P. Targeted Therapies for Parkinson's Disease: From Genetics to the Clinic. *Mov Disord* 2018;33(5):684-96. doi: 10.1002/mds.27414 [published Online First: 2018/04/29]
3. Impact of 98 LRRK2 variants linked to Parkinson's Disease on kinase activity and microtubule binding. 2022 doi: https://doi.org/10.1101/2022.04.01.486724
4. Alexia F Kalogeropulou EP, Francesca Tonelli, Sven M Lange, Melanie Wightman, Alan R Prescott, Shalini Padmanabhan, Esther Sammler, Dario R Alessi. Impact of 98 LRRK2 variants linked to

Parkinson's Disease on kinase activity and microtubule binding. *BioRxiv* 2022 doi: doi: https://doi.org/10.1101/2022.04.01.486724 [published Online First: 1 April 2022]

5. Erb ML, Moore DJ. LRRK2 and the Endolysosomal System in Parkinson's Disease. *J Parkinsons Dis* 2020;10(4):1271-91. doi: 10.3233/JPD-202138
6. Alessi DR, Sammler E. LRRK2 kinase in Parkinson's disease. *Science* 2018;360(6384):36-37. doi: 10.1126/science.aar5683 [published Online First: 2018/04/07]
7. Taylor M, Alessi DR. Advances in elucidating the function of leucine-rich repeat protein kinase-2 in normal cells and Parkinson's disease. *Curr Opin Cell Biol* 2020;63:102-13. doi: 10.1016/j.ceb.2020.01.001 [published Online First: 2020/02/10]
8. Bandres-Ciga S, Ahmed S, Sabir MS, et al. The Genetic Architecture of Parkinson Disease in Spain: Characterizing Population-Specific Risk, Differential Haplotype Structures, and Providing Etiologic Insight. *Mov Disord* 2019;34(12):1851-63. doi: 10.1002/mds.27864 [published Online First: 2019/10/30]
9. Fan Y, Howden AJM, Sarhan AR, et al. Interrogating Parkinson's disease LRRK2 kinase pathway activity by assessing Rab10 phosphorylation in human neutrophils. *Biochem J* 2018;475(1):23-44. doi: 10.1042/BCJ20170803 [published Online First: 2017/11/12]
10. Fan Y, Nirujogi RS, Garrido A, et al. R1441G but not G2019S mutation enhances LRRK2 mediated Rab10 phosphorylation in human peripheral blood neutrophils. *Acta Neuropathol* 2021;142(3):475-94. doi: 10.1007/s00401-021-02325-z [published Online First: 20210614]
11. Mir R, Tonelli F, Lis P, et al. The Parkinson's disease VPS35[D620N] mutation enhances LRRK2-mediated Rab protein phosphorylation in mouse and human. *Biochem J* 2018;475(11):1861-83. doi: 10.1042/BCJ20180248 [published Online First: 2018/05/11]
12. Lis P, Burel S, Steger M, et al. Development of phospho-specific Rab protein antibodies to monitor in vivo activity of the LRRK2 Parkinson's disease kinase. *Biochem J* 2018;475(1):1-22. doi: 10.1042/BCJ20170802 [published Online First: 2017/11/12]
13. Virreira Winter S, Karayel O, Strauss MT, et al. Urinary proteome profiling for stratifying patients with familial Parkinson's disease. *EMBO Mol Med* 2021;13(3):e13257. doi: 10.15252/emmm.202013257 [published Online First: 20210122]
14. Alcalay RN, Hsieh F, Tengstrand E, et al. Higher Urine bis(Monoacylglycerol)Phosphate Levels in LRRK2 G2019S Mutation Carriers: Implications for Therapeutic Development. *Mov Disord* 2020;35(1):134-41. doi: 10.1002/mds.27818 [published Online First: 2019/09/11]
15. Fuji RN, Flagella M, Baca M, et al. Effect of selective LRRK2 kinase inhibition on nonhuman primate lung. *Sci Transl Med* 2015;7(273):273ra15. doi: 10.1126/scitranslmed.aaa3634 [published Online First: 2015/02/06]
16. Jennings D, Huntwork-Rodriguez S, Henry AG, et al. Preclinical and clinical evaluation of the LRRK2 inhibitor DNL201 for Parkinson's disease. *Sci Transl Med* 2022;14(648):eabj2658. doi: 10.1126/scitranslmed.abj2658 [published Online First: 20220608]
17. Gruenberg J. Life in the lumen: The multivesicular endosome. *Traffic* 2020;21(1):76-93. doi: 10.1111/tra.12715
18. Zimprich A, Benet-Pages A, Struhal W, et al. A mutation in VPS35, encoding a subunit of the retromer complex, causes late-onset Parkinson disease. *Am J Hum Genet* 2011;89(1):168-75. doi: 10.1016/j.ajhg.2011.06.008
19. Lang TA, Altman DG. Basic statistical reporting for articles published in biomedical journals: the "Statistical Analyses and Methods in the Published Literature" or the SAMPL Guidelines. *Int J Nurs Stud* 2015;52(1):5-9. doi: 10.1016/j.ijnurstu.2014.09.006 [published Online First: 20140928]
20. Lis P, Burel S, Steger M, et al. Development of phospho-specific Rab protein antibodies to monitor in vivo activity of the LRRK2 Parkinson's disease kinase. *Biochem J* 2017 doi: 10.1042/BCJ20170802 [published Online First: 2017/11/12]

21. Fan Y, Nirujogi RS, Garrido A, et al. R1441G but not G201S mutation enhances LRRK2 mediated Rab10 phosphorylation in human peripheral blood neutrophils. *medRxiv* 2021:2021.01.28.21249614. doi: 10.1101/2021.01.28.21249614
22. Wang X, Negrou E, Maloney MT, et al. Understanding LRRK2 kinase activity in preclinical models and human subjects through quantitative analysis of LRRK2 and pT73 Rab10. *Sci Rep* 2021;11(1):12900. doi: 10.1038/s41598-021-91943-4 [published Online First: 20210618]
23. Alcalay RN, Hsieh F, Tengstrand E, et al. Higher Urine bis(Monoacylglycerol)Phosphate Levels in LRRK2 G2019S Mutation Carriers: Implications for Therapeutic Development. *Mov Disord* 2019 doi: 10.1002/mds.27818 [published Online First: 2019/09/11]
24. Ying Fan FT, Shalini Padmanabhan, Marco A.S. Baptista, Lindsey Riley, Danielle Smith, Connie Marras, Andrew Howden, Dario R. Alessi, Esther Sammler. Human peripheral blood neutrophil isolation for interrogating the Parkinson's associated LRRK2 kinase pathway by assessing Rab10 phosphorylation. *JoVE* 2019;in press
25. MacLeod DA, Rhinn H, Kuwahara T, et al. RAB7L1 interacts with LRRK2 to modify intraneuronal protein sorting and Parkinson's disease risk. *Neuron* 2013;77(3):425-39. doi: 10.1016/j.neuron.2012.11.033 [published Online First: 2013/02/12]
26. Riboldi GM, Di Fonzo AB. GBA, Gaucher Disease, and Parkinson's Disease: From Genetic to Clinic to New Therapeutic Approaches. *Cells* 2019;8(4) doi: 10.3390/cells8040364 [published Online First: 20190419]
27. Parkinson Progression Marker I. The Parkinson Progression Marker Initiative (PPMI). *Prog Neurobiol* 2011;95(4):629-35. doi: 10.1016/j.pneurobio.2011.09.005 [published Online First: 20110914]
28. Demirsoy S, Martin S, Motamedi S, et al. ATP13A2/PARK9 regulates endo-/lysosomal cargo sorting and proteostasis through a novel PI(3, 5)P2-mediated scaffolding function. *Hum Mol Genet* 2017;26(9):1656-69. doi: 10.1093/hmg/ddx070
29. Baptista MAS, Merchant K, Barrett T, et al. LRRK2 inhibitors induce reversible changes in nonhuman primate lungs without measurable pulmonary deficits. *Sci Transl Med* 2020;12(540) doi: 10.1126/scitranslmed.aav0820 [published Online First: 2020/04/24]

Acknowledgements: The work was supported by funding from the Michael J. Fox Foundation for Parkinson's Research [MJFF-020316, MJFF-009262]. ES was supported by a Chief Scientist Office Scottish Senior Clinical Academic Fellowship. We thank all patients and volunteers who have participated in this study. We acknowledge the excellent technical support of the MRC-Protein Phosphorylation and Ubiquitylation Unit (PPU) and MRC PPU Reagents and Services teams. We thank the Data Analysis Group at the School of Life Sciences at the University of Dundee for their useful discussion and guidance.

Author CRediT (Contributor Roles Taxonomy) Contribution: Conceptualization: ES, DRA, KMS. Data curation: SG and ES. Formal analysis: SG and ES. Funding acquisition: ES . Investigation: SG, AG, FT, JRM, AVA, HH, IC, VLM, TK, CH, Methodology: SG, FH, MS, ET, and ES. Project administration: ES. Resources: ET, MJM, JRM, VLM, WP, AZ and ES. Supervision: ES. Validation: SG, FH, MS, ET, KM, SP and ES. Writing- original draft: SG, and ES. Writing-review and editing: SG, AG, FT, ET, MJM, DRA, SP, JRM, AVA, HH, IC, VLM, TK, CH, FH, MS, ET, KM, WP, AZ, and ES

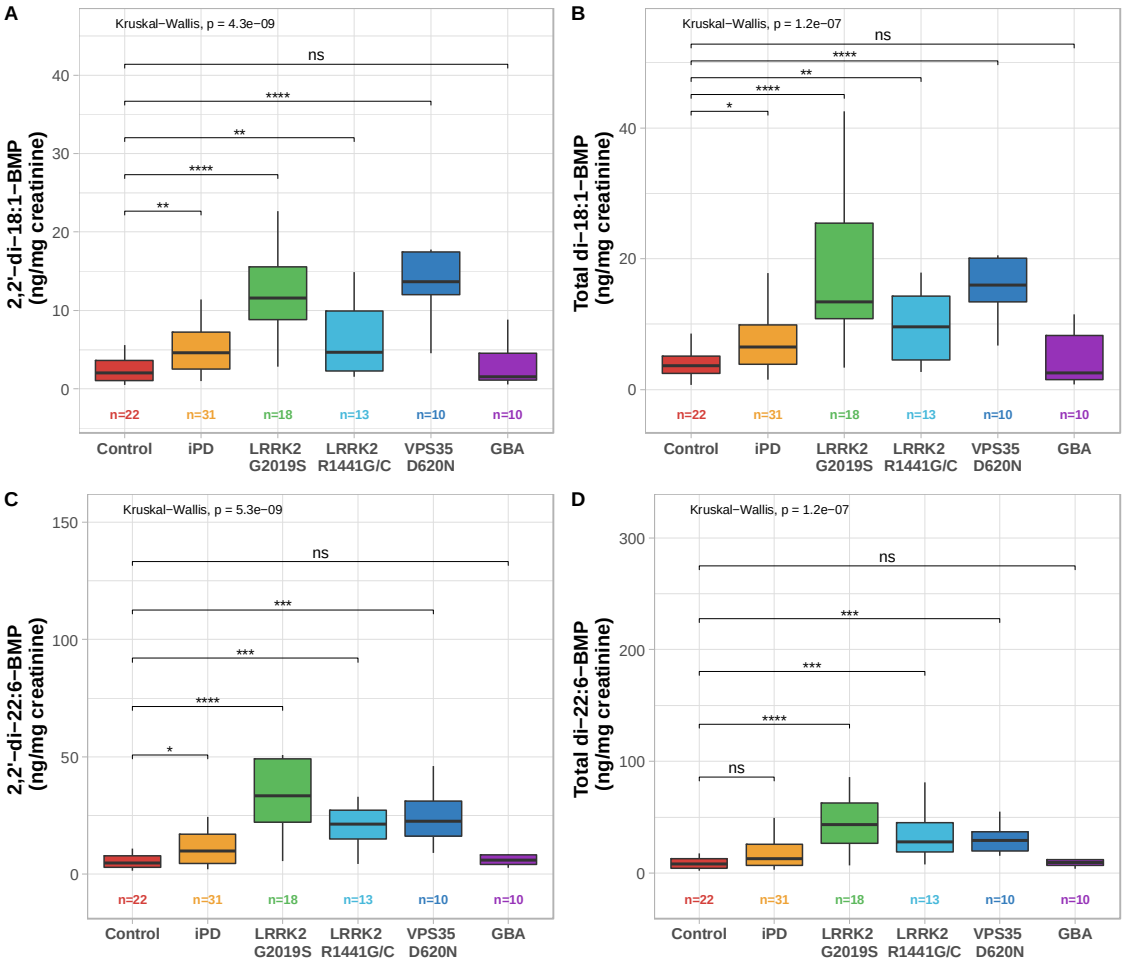

Is it maybe better to show violin type figures here where one can better see the spread of all of the data? The format of SFig2 where you can see all the dots for each replicate is better

Figure 1. Levels of urine BMP isoforms. Urine levels of **(A)** 2,2'-di-18:1-BMP, **(B)** total di-18:1-BMP, **(C)** 2,2'-di-22:6-BMP, and **(D)** total di-22:6-BMP expressed as ng of BMP per mg of creatinine are plotted per experimental group (indicated in the x-axis), in boxplots. Individual datapoints are shown, with triangle shapes indicating non-manifesting mutation carriers. Statistically significant differences between experimental groups were assessed with Kruskal-Wallis test, and overall p-values are displayed on the plots. Post-hoc Dunn's multiple comparison test was employed to identify groups significantly different from control (*$p < 0.05$, **$p < 0.01$, ***$p < 0.001$, ****$p < 0.0001$).

Table 1. Demographic information and urine BMP levels in study participants.

	Control	iPD	LRRK2 G2019S	LRRK2 R1441G/C	VPS35 D620N	GBA	*p*-value
	N = 22	*N = 31*	*N = 18*	*N = 13*	*N = 10*	*N = 10*	
Age median (range)	55.00 (24.00, 71.00)	65.50 (45.00, 88.00)	59.50 (42.00, 81.00)	65.00 (50.00, 83.00)	62.50 (29.00, 76.00)	61.00 (49.00, 64.00)	<0.001[1]
Sex female/male	11/11	15/16	11/7	6/7	7/3	3/7	0.5[2]
PD status PD/NMC	--	--	11/7	7/6	9/1	10/0	--
Total di-18:1-BMP median (range)	3.66 (0.72, 8.54)	6.48* (1.48, 38.88)	13.43**** (3.30, 42.56)	9.57** (2.70, 34.68)	15.97**** (6.71, 55.37)	2.56 (0.80, 45.53)	<0.001[1]
2,2'-di-18:1-BMP median (range)	2.04 (0.52, 5.60)	4.58** (1.01, 34.58)	11.59**** (2.86, 33.59)	4.68** (1.55, 29.59)	13.69**** (4.54, 46.10)	1.58 (0.59, 21.59)	<0.001[1]
Total 22:6-BMP median (range)	8.33 (2.18, 41.14)	12.84 (3.28, 104.92)	43.52**** (6.98, 321.98)	28.11*** (7.94, 81.34)	29.19*** (15.51, 162.36)	9.66 (3.97, 34.21)	<0.001[1]
2,2'-di-22:6-BMP median (range)	4.83 (1.47, 19.59)	9.86* (2.17, 60.15)	33.43**** (5.61, 153.74)	21.27*** (4.35, 47.35)	22.61*** (8.98, 126.35)	5.93 (2.81, 21.31)	<0.001[1]

Values are median of the measured BMP normalized to the creatinine amount (ng/mg creatinine).

[1] Kruskal-Wallis rank sum test.

[2] Fisher's exact test.

Values significantly different from Control group: *$p < 0.05$; **$p < 0.01$; ***$p < 0.001$, ****$p < 0.0001$, Dunn's multiple comparison test.

NMC: non-manifesting carrier.

GBA group includes carriers of the following variants: c.762-1G>C, het.del-from exon3, p.Pro138Leufs*62, p.Thr408Met, p.Ser212* and p.Thr408Met, p.Glu365Lys, p.Asn409Ser.

Table 2. Levels of urine BMPs for the extended panel.

	Control		iPD		LRRK2 G2019S		LRRK2 R1441G/C		VPS35 D620N		GBA		p-value[1]
	median (range)	*N*	*median (range)*	*N*	*median (range)*	*N*	*median (range)*	*N*	*median (range)*	*N*	*median (range)*	*N*	
BMP 18:1/22:6	5.19 (1.86, 22.99)	22	10.38* (2.92, 56.06)	31	32.40*** (12.75, 168.50	18	19.42*** (5.80, 53.00)	13	25.37*** (8.59, 146.41)	10	3.87 (1.74, 48.30)	10	<0.001
BMP 18:2	2.02 (0.72, 6.25)	22	2.97* (0.95, 29.79)	31	9.88*** (2.08, 136.82)	18	9.01*** (2.20, 27.02)	13	16.67*** (5.98, 42.34)	10	1.97 (0.95, 9.82)	10	<0.001
BMP 18:1/18:2	4.57 (1.14, 15.29)	22	8.07* (2.16, 58.99)	31	23.98*** (5.66, 157.33)	18	18.60*** (4.40, 46.40)	13	28.19*** (9.83, 89.80)	10	3.48 (1.63, 53.08)	10	<0.001
BMP 18:2/22:6	1.94 (0.77, 7.56)	20	3.51* (1.25, 18.31)	31	13.70*** (4.72, 108.74)	18	8.08*** (4.13, 26.27)	13	12.98*** (5.17, 53.91)	10	1.92 (0.89, 8.00)	10	<0.001
2,3'-BMP 18:1[3]	1.43 (0.43, 4.04)	14	3.88 (0.78, 11.75)	9	9.73 (3.31, 16.15)	2	2.21 (1.41, 6.56)	7	NA	0	1.39 (0.40, 17.42)	6	0.074
2,3'-BMP 22:6[3]	3.81 (0.96, 16.42)	14	10.15 (2.27, 37.03)	9	82.42* (29.50, 135.33)	2	16.22 (3.27, 29.80)	7	NA	0	3.93 (1.78, 11.63)	6	0.013
3,3'-BMP 22:6[3]	0.60 (0.08, 5.13)	14	0.84 (0.17, 7.75)	9	22.32* (11.73, 32.91)	2	1.70 (0.42, 4.19)	7	NA	0	0.53 (0.15, 1.27)	6	0.019
BMP 20:4/22:6	0.48 (0.27, 1.94)	12	0.65 (0.21, 4.93)	25	2.13*** (0.53, 19.57)	18	1.61** (0.52, 6.04)	12	2.66*** (1.31, 16.10)	10	0.70 (0.23, 2.21)	6	<0.001
BMP 18:2/20:4	0.31 (0.15, 1.40)	10	0.47 (0.19, 4.03)	26	1.31** (0.44, 13.64)	17	1.32 (0.27, 4.53)	12	2.50*** (1.02, 10.64)	10	0.72 (0.11, 2.09)	7	<0.001
BMP 16:0/18:2	0.30 (0.19, 0.82)	9	0.36 (0.09, 4.23)	24	1.07** (0.35, 6.13)	17	1.00** (0.42, 3.06)	11	1.72*** (0.58, 5.87)	10	0.67 (0.17, 3.10)	6	<0.001
3,3'-BMP 18:1[3]	0.37 (0.04, 1.79)	9	1.09 (0.80, 6.09)	6	5.42 (0.22, 10.63)	2	1.65 (0.19, 3.05)	5	NA	0	0.48 (0.27, 6.53)	3	0.2
BMP 16:0/18:1[2]	0.71 (0.17, 1.02)	8	0.71 (0.15, 3.87)	22	2.19** (0.55, 6.06)	16	1.96* (0.81, 5.44)	6	3.64*** (1.38, 17.82)	10	0.41 (0.30, 2.36)	4	<0.001
Lyso-BMP 22:6[2]	0.11 (0.04, 0.30)	8	0.18 (0.10, 0.93)	22	0.50** (0.13, 1.49)	16	0.41* (0.20, 0.61)	6	0.52** (0.21, 1.89)	10	0.39 (0.10, 0.66)	4	<0.001
Lyso-BMP 18:1[2]	0.25 (0.20, 0.71)	8	0.38 (0.12, 2.10)	22	0.75* (0.25, 1.85)	16	0.76* (0.39, 1.29)	6	0.83** (0.42, 3.39)	10	0.59 (0.10, 2.21)	4	0.001
BMP 20:3/22:6[2]	0.35 (0.20,	8	0.69 (0.23,	22	2.03*** (0.67,	16	1.24* (0.66,	6	2.62*** (1.29,	10	0.45 (0.18,	4	<0.001

	0.45)		3.11)		10.07)		2.60)		11.42)		0.72)		
BMP 18:0/20:4[2]	0.07 (0.07, 0.08)	2	0.07 (0.05, 0.19)	9	0.12 (0.08, 0.59)	8	NA	0	0.19 (0.09, 1.25)	9	0.28	1	0.015

Values are median of the measured BMP normalized to the creatinine amount (ng/mg creatinine).
[1]Kruskal-Wallis rank sum test
[2]Only measured for 2019 batch
[3]Only measured in 2021 batch
Values significantly different from Control group: *$p < 0.05$; **$p < 0.01$; ***$p < 0.001$, Dunn's multiple comparison test.

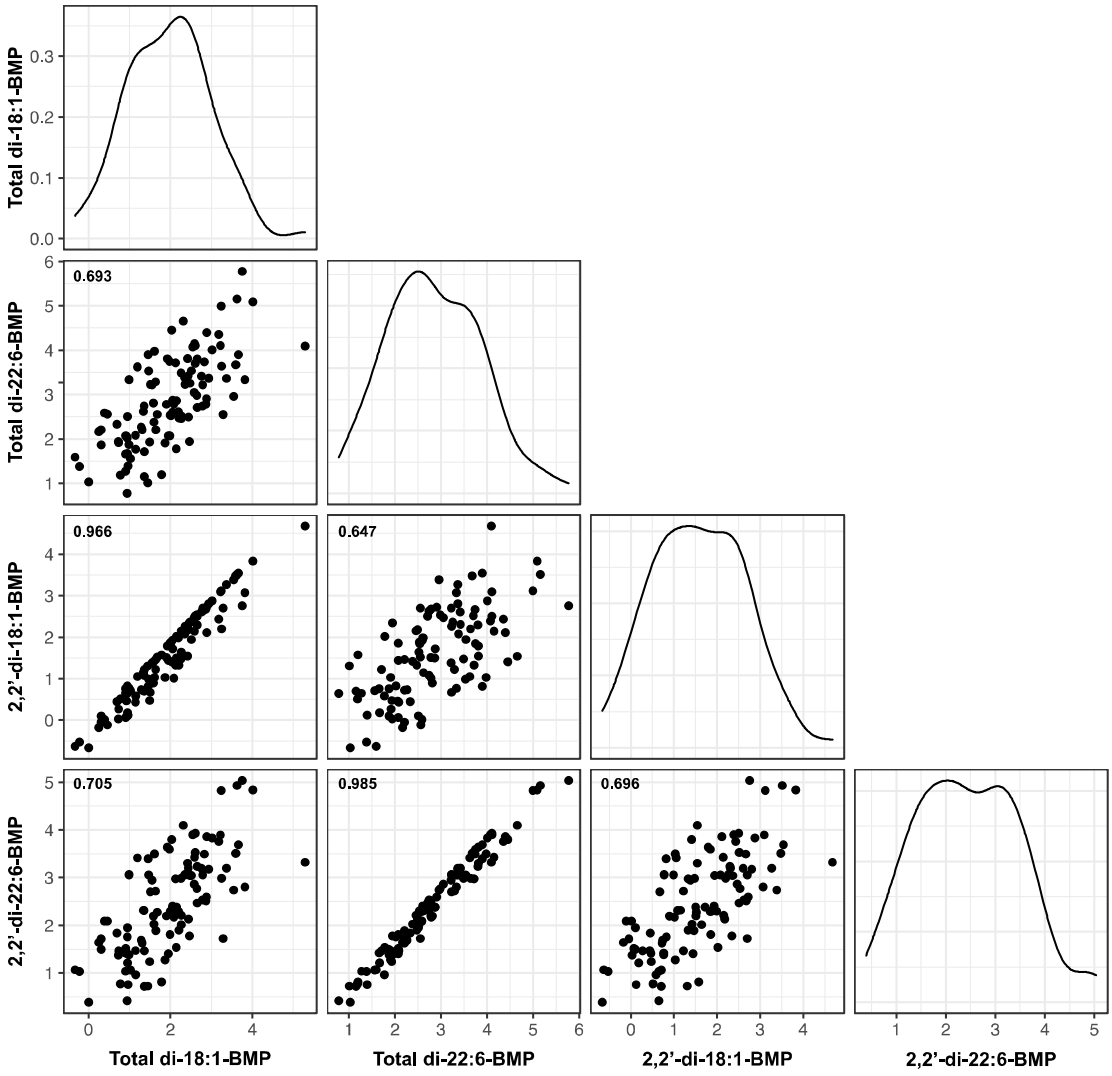

Supplementary figure 1. Correlation between main urine BMP species. The values for 2,2'- and total di-18:1- and di-22:6-BMP were log-transformed and plotted in a scatterplot matrix to assess correlation between pairs of individual BMP species. The diagonal shows the histograms of the log-transformed BMP values that now follow an approximately normal distribution. The Pearson correlation coefficient is displayed on the top left corner of each scatterplot.

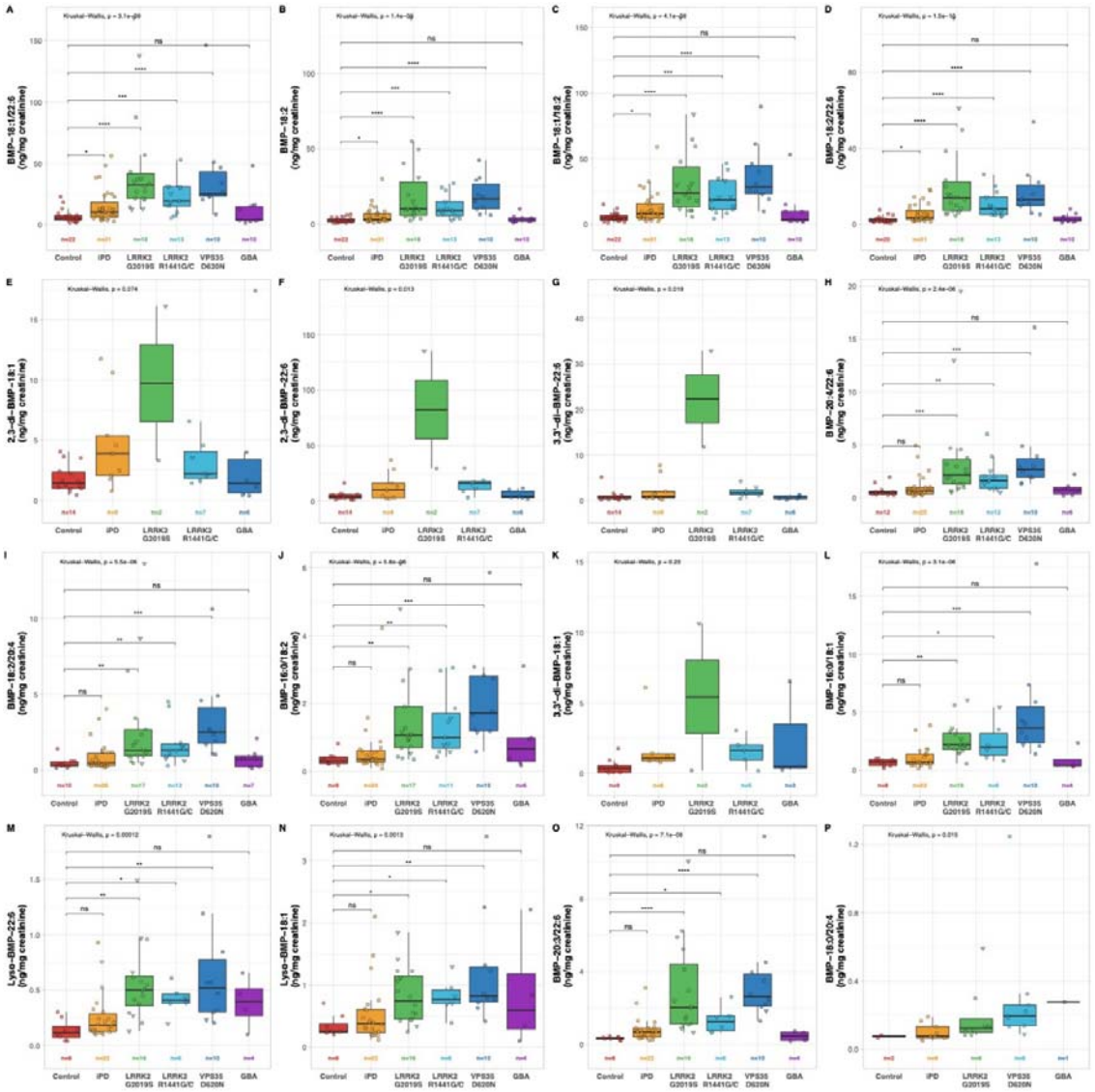

Supplementary figure 2. Levels of urine BMP isoforms for the extended panel. Urine levels of **(A)** BMP-18:1/22:6, **(B)** BMP-18:2, **(C)** BMP-18:1/18:2, **(D)** BMP-18:2/22:6, **(E)** 2,3'-BMP-18:1, **(F)** 2,3'-BMP-22:6, **(G)** 3,3'-BMP-22:6, **(H)** BMP-20:4/22:6, **(I)** BMP-18:2/20:4, **(J)** BMP-16:0/18:2, **(K)** 3,3'-BMP-18:1, **(L)** BMP-16:0/18:1, **(M)** Lyso-BMP-22:6, **(N)** Lyso-BMP-18:1, **(O)** BMP-20:3/22:6, **(P)** BMP-18:0/20:4, expressed as ng of BMP-per mg of creatinine, are plotted per experimental group (indicated in the x-axis), in boxplots. Individual datapoints are shown, with triangle shapes indicating non-manifesting mutation carriers. Group size is indicated. Statistically significant differences between experimental groups were assessed with Kruskal-Wallis test, and overall p-values are displayed on the top left corner of each plot. Post-hoc Dunn's multiple comparison test was employed to identify groups significantly different from control (*$p < 0.05$, **$p < 0.01$, ***$p < 0.001$, ****$p < 0.0001$), except in cases where overall $p > 0.05$ or group size ≤ 2.

Supplementary table 1. Participant demographic and clinical characteristics. For each participant, sample collection site is provided as: BCN (Barcelona), VIE (Vienna), DND (Dundee), or SSB (San Sebastian). Also provided are age at study participation, age at PD diagnosis (where applicable), sex (M, for male, and F, for female), experimental group (control, iPD – idiopathic PD –, LRRK2 G2019S, LRRK2 R1441G/C, VPS35 D620N, GBA, or other), and PD status (NMC for non-manifesting mutation carriers, or PD). Other details including additional mutations are listed in the comments column, where applicable. Values for all measured BMP species presented as ng of BMP per mg of creatinine are provided. BQL designates BMP levels that were below quantification level and NM designates values that were not measured for a particular individual.

Supplementary table 2. Comparison between PD-manifesting and non-manifesting LRRK2 mutation carriers for main urine BMP isoforms. Summary of the adjusted p-values and significance level for the comparison between PD-manifesting (PD) and non-manifesting (NMC) carriers of LRRK2 G2019S or LRRK2 R1441G/C mutations, for the four main urine BMP species. Kruskal-Wallis test, with post-hoc Dunn's multiple comparison test (ns: non-significant, $p > 0.05$).

Supplementary table 3. Multiple group comparison for main urine BMP isoforms. Summary of the adjusted p-values and significance level for the comparisons between the 5 experimental groups (control, iPD – idiopathic PD –, LRRK2 G2019S, LRRK2 R1441G/C, VPS35 D620N, and GBA), for the four main urine BMP species. Kruskal-Wallis test, with post-hoc Dunn's multiple comparison test (*$p < 0.05$, **$p < 0.01$, ***$p < 0.001$, ****$p < 0.0001$, ns: non-significant, $p > 0.05$).